JOURNAL OF CATALYSIS 104, 279–287 (1987)

CO-Induced Disintegration of Rhodium Aggregates Supported in Zeolites: *In Situ* Synthesis of Rhodium Carbonyl Clusters

G. BERGERET, P. GALLEZOT,[1] P. GELIN, Y. BEN TAARIT, F. LEFEBVRE, C. NACCACHE, AND R. D. SHANNON[2]

Institut de Recherches sur la Catalyse,[3] 2 Avenue Albert Einstein, 69626 Villeurbanne Cédex, France

Received December 10, 1985; revised October 31, 1986

Y-type zeolites exchanged with $[Rh(NH_3)_5Cl]^{2+}$ ions and subjected to different treatments have been studied by radial electron distribution derived from X-ray scattering and by infrared spectroscopy. O_2 treatment at 620 K of the RhY zeolite leads to rhodium oxide clusters and rhodium cations. Metal aggregates smaller than 1 nm are formed upon H_2 reduction at 470 K. The adsorption of CO at 300 K produces a complete disintegration of the Rh aggregates into monomeric species identified as $Rh^I(CO)_2$ by IR spectroscopy. In the presence of $CO:H_2O$ mixture, the $Rh^I(CO)_2$ species condense into polynuclear carbonyl clusters.

INTRODUCTION

Considerable attention has been paid in the past few years to the atomic structure of metal aggregates encaged in zeolites (*1–5*). Using radial electron distribution (RED) calculated from X-ray scattering data, it has been shown that the structure of 1-nm Pt aggregates depends upon the binding energy of the adsorbates. Thus CO adsorption (*4*) or dissociative hydrocarbon chemisorption (*3*) induces a disorder in the structure of the aggregates because the formation of Pt–C bonds displaces the Pt atoms from their equilibrium positions. These chemisorptions, although they are corrosive, do not lead to complete cluster disintegration such as that observed upon NO adsorption at 300 K on 2-nm Pd aggregates in Y zeolites (*6*).

It has been shown (*7, 8*) that Rh aggregates with a narrow size distribution centered below 1 nm can be prepared by proper treatments of Y zeolites exchanged with $[Rh(NH_3)_5Cl]^{2+}$ ions. Primet (*8*) has shown by IR spectroscopy that CO adsorption on small Rh particles leads to $Rh^I(CO)_2$ species. It has been demonstrated by EXAFS that Rh aggregates supported on alumina (*9–11*) or TiO_2 (*12*) are partially disrupted into isolated $Rh^I(CO)_2$ upon CO adsorption, the higher the dispersion, the lower the fraction of Rh atoms remaining metallic. A recent IR study (*13*) supports these previous findings (*8–11*).

The aim of the present work is to determine if the Rh aggregates hosted in the zeolite cages can be disintegrated completely upon CO adsorption. Moreover, it has been shown by IR spectroscopy that supported rhodium carbonyl clusters can be synthesized from $Rh^{III}Y$ zeolite in the course of the CO + H_2 reaction (*14*) or from $Rh^I(CO)_2$ species adsorbed on alumina (*15*). Recently we were able to prepare Rh carbonyl clusters from $Rh^{III}Y$ zeolites and to characterize them by IR and ^{13}C NMR spectroscopies (*16, 17*). Direct evidence for the formation of Rh–Rh bonds characteristic of polynuclear carbonyl clusters was also obtained by a RED study (*18*). Therefore the second aim of this study is to detect by RED the appearance of new Rh–Rh bonds

[1] To whom correspondence should be addressed.

[2] On leave from Central Research and Development Dept., E.I. du Pont de Nemours and Co., Wilmington, DE 19898.

[3] Laboratoire propre du CNRS, conventionné à l'Université Claude Bernard Lyon I, France.

0021-9517/87 $3.00

TABLE 1

Treatment of Rhodium Zeolites

Sample	Treatment[a]
$RhY(O_2)$	$[Rh(NH_3)_5Cl]^{2+}$-exchanged Y zeolite; heated from 300 to 620 K under flowing O_2 (0.5 K/min); kept 30 min at 620 K, evacuated 300 K (kept under Ar)
$RhY(H_2)$	$RhY(O_2)$ evacuated at 300 K; heated in flowing H_2 from 300 to 470 K (2 K/min); kept 30 min at 470 K; cooled to 300 K under H_2 (kept under H_2)
RhY(CO)	$RhY(H_2)$ evacuated at 300 K; contacted with 200 Torr of CO and 560 Torr of Ar at 300 K (kept under CO : Ar)
$RhY(CO + H_2O)$	RhY(CO) evacuated at 300 K; contacted at 300 K with 15 Torr of H_2O vapor (30 min); contacted at 300 K with 760 Torr of CO (kept under $CO : H_2O$)

Note. 1 Torr = 133.3 N m^{-2}

[a] Atmosphere during X-ray collection at 300 K is in parentheses.

at the expense of the species resulting from the Rh aggregate disintegration so that the complete transformation of metal aggregates into carbonyl clusters can be demonstrated.

EXPERIMENTAL

The RhY zeolite was prepared from NaY (LZY-52, Union Carbide) by ion exchange in 800 cm^3 of 0.001 *M* $[Rh(NH_3)_5Cl]Cl_2$ solution per gram of zeolite at 350 K for 12 h, washing free of Cl^- ions, centrifuging, and drying at 380 K. The unit cell composition determined by chemical analysis on calcined powder was $Rh_{11.3}Na_{16.5}H_{6.6}Si_{135}Al_{57}O_{384}$.

The exchanged RhY zeolite was activated in a U-shaped quartz cell equipped with two 5-cm^2 frits. One gram of zeolite was heated in flowing O_2 at 0.5 K/min from 300 to 623 K with oxygen flowing upward at 5 liters/min to produce a nearly fluidized bed. After evacuation of O_2 at 300 K, the zeolite was reduced in flowing H_2 (0.5 liter/min) from 300 to 470 K at 2 K/min, kept at 470 K for 30 min, and cooled under H_2. It was checked by transmission electron microscopy on ultramicrotome cuts of zeolites that the Rh aggregates formed upon reduction are smaller than 1 nm in diameter in agreement with previous findings (*7, 8*). It should be stressed that the activation treatment in O_2 prior to H_2 reduction is essential to obtain a good final dispersion. It must be conducted with good contact between the gas and solid phase and with a slow heating rate; otherwise, an autoreduction process can result in a heterogeneous dispersion.

The quartz cell was opened in a glovebox flushed with O_2-free Ar. The zeolite powder (1 g) was pressed into the rectangular cavity of a sample holder and placed in a controlled atmosphere cell equipped with a beryllium window enabling the diffraction pattern to be recorded. The treatments under CO or $CO : H_2O$ were performed in this cell connected to a gas and vacuum line. Table 1 summarizes the treatment conditions.

Collection of X-ray intensities, data reduction, and Fourier transform were performed as described in previous work (*1–4*). The radial distribution, $4\pi r^2\rho(r)$, of a

dehydrated NaHY zeolite was subtracted from the radial distribution of the RhY zeolites. Note that the X-ray data collection was started only after the X-ray diffraction pattern did not exhibit any further change with time, which took 1 day for RhY (CO + H_2O) (see Section 4 of the discussion).

For infrared studies, a less-rhodium-exchanged sample was prepared following the same procedure. The rhodium Y zeolite contained four rhodium atoms per unit cell (3.5 wt% of Rh). Infrared absorption spectra were obtained for a zeolite mass of about 12 mg. The powder, compressed as a disk of 18 mm in diameter, was introduced into a Pyrex sample holder. Treatments were made in a greaseless cell equipped with two CaF_2 windows. IR spectra were recorded using a Perkin–Elmer 580 spectrometer with a slit width giving a resolution of 2.8 cm^{-1}. Treatments were as similar as possible to those described for the sample studied by RED: heated in flowing O_2 at 0.5 K/min from 300 to 623 K, O_2 evacuated at 300 K, reducted in H_2 flowing from 300 to 470 K at 2 K/min, kept at 470 K for 30 min, and cooled under H_2.

RESULTS AND DISCUSSION

The radial electron distributions of the Rh zeolites are given in Fig. 1. Previous investigations (*1–4*) on Pt aggregates have shown that the RED gives primarily metal–metal distances because the peak intensities are proportional to Z^2 which heavily weights those atoms with high atomic numbers. However, Z^2(Rh) is much smaller than Z^2(Pt) so that the distances between rhodium and light atoms could possibly be detected. The distributions are expected to be plagued by oscillations which might be real interatomic distances, e.g., between Rh atoms and the framework oxygen anions or false maxima coming from the Fourier transform procedure. As expected, the distributions given in Figs. 1 and 3 are much noisier than Pt distributions obtained previously (*1–4*). Although a number of small peaks could possibly be interpreted by comparison with interatomic distances calculated from models, we shall focus our attention on the most prominent peaks of the distributions which are determined with a ±0.02 Å (1 Å = 0.1 nm) accuracy.

1. Structure of the Oxidized Sample RhY(O_2)

The RED of RhY(O_2) obtained by heating $Rh(NH_3)_5Cl$ Y in O_2 at 620 K is given in Fig. 1a. A sample heated only to 573 K gave a similar spectrum (*18*). There are many peaks above 4 Å which might correspond to distances between Rh ions in different cationic sites and to Rh–framework oxygen distances. The largest peak at 3.11 Å corre-

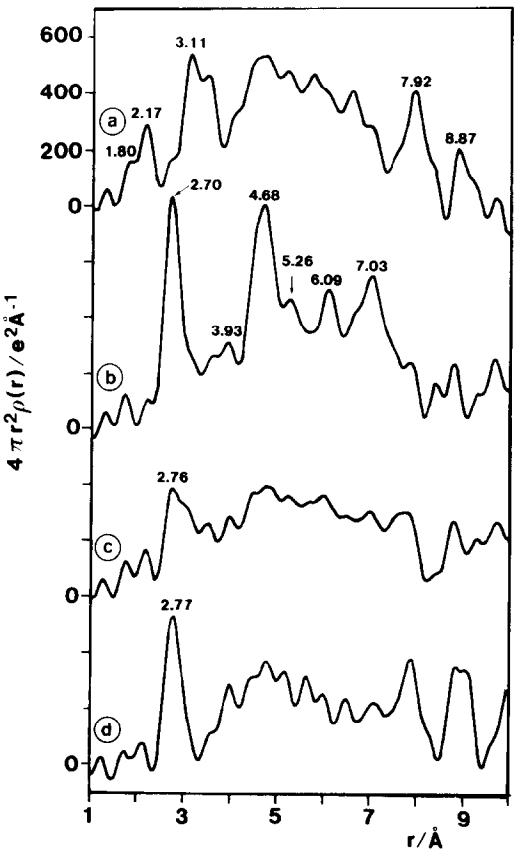

FIG. 1. Radial electron distribution of the $Rh_{11.3}Na_{16.5}Y$ zeolite; the RED of a Rh-free NaHY support has been subtracted; (a) RhY(O_2); (b) RhY(H_2); (c) RhY(CO); (d) RhY(CO + H_2O); see Table 1 for corresponding treatments.

TABLE 2

Significant Interatomic Distances in Encaged Rh Species

Sample	Distances (Å)
$RhY(O_2)$	3.11: Rh–Rh in dimeric oxide
$RhY(H_2)$	2.70, 3.93, 4.68, 5.26, 6.09, 7.03: Rh–Rh metal–metal bonds in fcc Rh aggregates; 2.689, 3.803, 4.658, 5.378, 6.013, 7.115 corresponding Rh–Rh distances in bulk Rh metal
RhY(CO)	2.76: Rh–Rh bond in Rh carbonyl clusters
$RhY(CO + H_2O)$	2.77: Rh–Rh bond in Rh carbonyl clusters ($Rh_6(CO)_{16}$)

sponds probably to the distances between Rh ions bridged by extra-framework oxygen anions. Although the Rh–Rh distances in bulk rhodium oxides are somewhat smaller (2.72 and 3.03 Å in Rh_2O_3, form I (*19*), and 3.09 Å in RhO_2 (*20*)), one may expect that small oxide clusters (dimer or trimer) exhibit different bond lengths from the bulk oxides. Also, the peaks at 1.8 and 2.17 Å could correspond to Rh–O_t (terminal oxygen) and Rh–O_{br} (bridging oxygen), respectively, whereas the Rh–O distance in bulk RhO_2 (1.98 Å) is between these values. The formation of rhodium oxide clusters in oxidized RhY zeolite was also reported by Van Brabant *et al.* (*21*). Because the intensity of the 3.11-Å peak is not very high, some Rh ions might not be involved in oxide clusters but rather occupy the zeolite cation sites. The peaks at 7.92 and 8.87 Å probably correspond to distances between these cation sites.

2. *Structure of the Rhodium Metal Aggregates*

The RED of zeolite $RhY(H_2)$ obtained by H_2 reduction of $RhY(O_2)$ is given in Fig. 1b. The strong peaks appearing at 2.70 and 4.68 Å are in fair agreement with the first and third Rh–Rh distances in bulk fcc rhodium (2.689 and 4.658 Å, respectively, Table 2). The other peaks at 3.93, 5.26, 6.09, and 7.03 Å also correspond to fcc rhodium (see Table 2) but the distances are contracted or elongated with respect to the normal bulk values. Distortion was reported previously for bare Pt aggregates (*2, 22*) but their structure was ordered once covered by H_2, whereas the Rh aggregates are distorted even under H_2 which means that the H_2 adsorption does not produce a complete structure relaxation. This could be due to the smaller size of the Rh aggregates since distortion is expected to increase when the number of atoms in the aggregates decreases. Indeed, electron microscopy indicates that the Rh aggregates are smaller than the Pt aggregates.

The peak positions are perturbed by the presence of a broad band in the distance range 3–7 Å. This is probably caused by the combination of a large number of peaks corresponding to the interatomic distances between the rhodium and the framework atoms of the cage walls, which are also observed in the other radial distributions (Figs. 1a, 1c, 1d, 3).

3. *Disintegration of the Rhodium Aggregates*

Figure 1c shows the result of the reaction of CO at 300 K with the Rh aggregates. The complete disappearance of all the Rh–Rh bonds characteristic of the metal is especially striking. The sole prominent feature is a weak peak at 2.76 Å. Clearly all the Rh–Rh metal bonds have been broken so that

the rhodium is now in the form of monomeric species.

The infrared spectrum of the reduced sample shows no absorption in the range 2500–1600 cm^{-1} (Fig. 2a) other than the zeolite background. However, after CO adsorption at 300 K, many bands are detected in the C–O vibration range (Fig. 2b). These bands are due to carbon monoxide adsorbed on metal (ν_{CO} = 2060 and 1874 cm^{-1}) (*7*), to rhodium(I) dicarbonyl species (ν_{CO} = 2116–2048 cm^{-1}, 2101–2022 cm^{-1}) (*7*, *8*) and the last ones, relatively weak, to rhodium clusters (ν_{CO} = 1830 and 1760 cm^{-1}) (*17*) (Table 3). The IR spectrum is modified with time, and the CO bands of monovalent carbonyl rhodium complexes increase while those of CO on metal decrease.

In order to provide clear evidence that the CO bands at 2116, 2101, 2048, and 2022 cm^{-1} derive from an oxidation process of rhodium in the presence of carbon monoxide, a characteristic reaction of $Rh^{I}(CO)_2$ was studied on this sample. Rhodium(I) di-

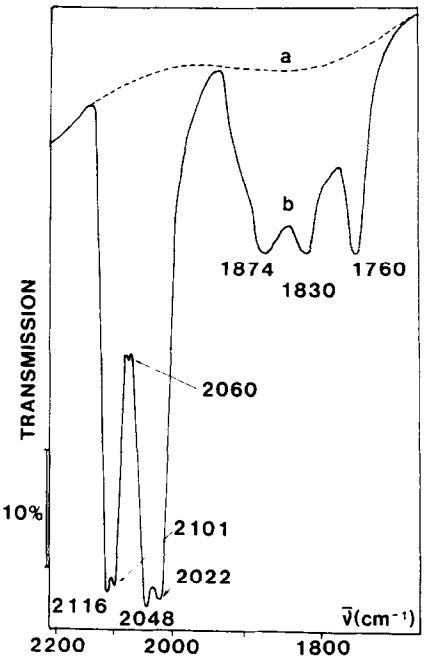

FIG. 2. Infrared spectra of the RhY zeolite; (a) after treatment under H_2 and vacuum at 470 K and (b) after adsorption of CO at 300 K ($P \approx 10$ Torr).

TABLE 3

ν_{CO} Frequencies of Some Rhodium Carbonyls Entrapped within Y Zeolite

Species	ν_{CO} (cm^{-1})
$Rh^{(0)}$–CO	2060(vs)
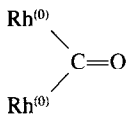	1874(s)
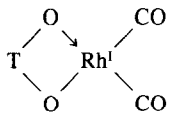	2101(vs), 2022(vs)
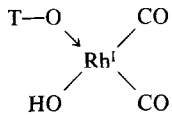	2116(vs), 2048(vs)
$Rh_4(CO)_{12}$ (dehydrated zeolite)	2130(w), 2090(vs), 2060(w), 1875(w), 1830(s)
$Rh_4(CO)_{12}$ (hydrated zeolite)	2120(w), 2080(vs), 2030(w), 1930(w), 1870(s)
$Rh_6(CO)_{16}$ (dehydrated zeolite)	2135(w), 2095(vs), 2070(w), 2045(w), 1760(s)
$Rh_6(CO)_{16}$ (hydrated zeolite)	2086(vs), 1800(s)

Note. T = Al, Si.

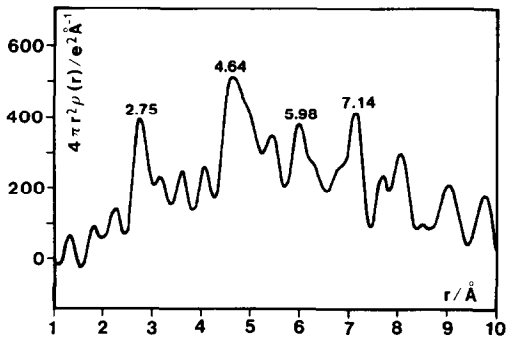

FIG. 3. Radial electron distribution. Effect of CO on $Rh_{11.3}Na_{16.5}Y$ zeolite containing a bimodal distribution of rhodium particles (1 and 3 nm).

carbonyl synthesized in Y zeolite is known to add CH_3I oxidatively, forming a trivalent acetyl carbonyl rhodium complex characterized by IR ν_{CO} bands at 2090 and 1720 cm^{-1} (*23*). The IR spectrum observed is quite similar to that of the trivalent acetyl rhodium complex and confirms the presence of a monovalent rhodium dicarbonyl.

To sum up, it can be concluded from IR and RED measurements that rhodium aggregates in Y zeolites become disintegrated and oxidized when CO is adsorbed, leading to the formation of rhodium(I) dicarbonyl monomers when CO is adsorbed. This is in agreement with previous EXAFS studies on Rh/Al_2O_3 and Rh/TiO_2 catalysts (*9–12*).

The small peak at about 2.76 Å in the RED (Fig. 1c) corresponds to the formation of new Rh–Rh bonds different from those present in the metal. This indicates that polynuclear carbonyl species have been formed. The nature and development of this process is discussed in the following section. The other weak peaks in the range 3–7 Å could correspond to Rh–framework atom distances.

As shown previously in the case of Rh/Al_2O_3 (*10*) and Rh/TiO_2 (*12*) catalysts, the CO-induced disintegration of rhodium metal may be incomplete. Thus, a RED study was performed on a rhodium zeolite activated under less stringent conditions than those described in Table 1 for $RhY(O_2)$. A transmission electron microscopic investigation carried out after reduction showed that the dispersion of rhodium is bimodal, with maxima at 1 and 3 nm. Figure 3 gives the distribution obtained after contacting the reduced sample with CO under the same conditions as those yielding RhY(CO) (Table 1). It is noteworthy that this distribution still exhibits Rh–Rh metal distances in contrast with that of RhY(CO) (Fig. 1c) involving clusters small than 1 nm. Therefore the disintegration of Rh aggregates induced by CO at room temperature proceeds to completion only if the aggregates are small enough, as noticed earlier on Rh/Al_2O_3 (*9–11*) and Rh/TiO_2 (*12*) catalysts. Indeed, low-coordinate atoms are expected to be more easily extracted by the CO chemisorption which is the first step of the disintegration process. Also CO dissociation favoring the oxidation of Rh^0 in Rh^I could be easier on the smaller aggregates, as suggested previously (*11*).

4. In Situ Synthesis of Carbonyl Clusters

It has been shown (*16*) that the IR spectrum of a RhY zeolite containing $Rh^I(CO)_2$ species, treated under a $CO:H_2O$ mixture, shows a change with time: the characteristic bands of rhodium(I) dicarbonyl species decrease while new ν_{CO} bands due to $Rh_4(CO)_{12}$ and $Rh_6(CO)_{16}$ develop. Especially, two bands characteristic of bridged CO were detected at 1870 and 1800 cm^{-1}, due, respectively, to $Rh_4(CO)_{12}$ and $Rh_6(CO)_{16}$ solvated by water molecules. The spectrum changed with time and finally only the $Rh_6(CO)_{16}$ bands were observed.

After contacting the RhY(CO) sample with the $CO:H_2O$ mixture (Table 1), the X-ray pattern was recorded after successive periods of time. The pattern changed continuously during the first day of exposure. Especially the intensities of the 111, 220, and 311 zeolite diffraction lines, which are very sensitive to scattering matter in extra-framework positions, changed continuously with time. This indicates that the encaged $Rh^I(CO)_2$ species migrate progres-

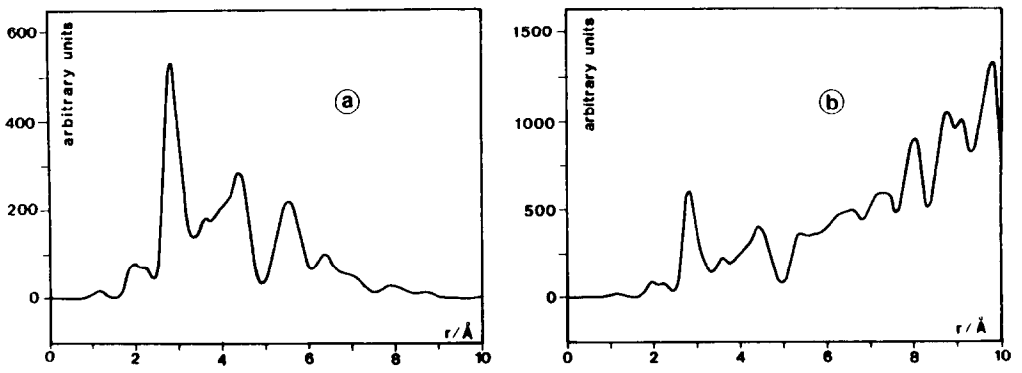

FIG. 4. Calculated radial electron distribution using the computer program RADMOR (*27*) and the atomic coordinates in the crystal structure of $Rh_6(CO)_{16}$ (*28*); (a) isolated $Rh_6(CO)_{16}$ cluster; (b) 12 unit cells (48 associated $Rh_6(CO)_{16}$ clusters).

sively in the porous zeolite network until they form the rhodium clusters. Because of these modifications, the X-ray data used to calculate the RED of RhY(CO + H_2O) were recorded 2 days after exposure to the CO : H_2O mixture.

Figure 1d shows the RED obtained after contacting RhY(CO) with a mixture of CO and H_2O at 300 K (Table 1). The predominant feature of the RED is a strong peak at 2.77 Å. It demonstrates that new Rh–Rh bonds have been formed probably at the expense of the monomeric species derived from the Rh aggregate disintegration. The presence of metal aggregates can be eliminated on the basis of the peak maximum at 2.77 Å instead of 2.69 Å, a difference much higher than the error on distance, and of the absence of any other metal–metal distances similar to those appearing in Fig. 1b. Instead it can be concluded that the 2.77-Å peak is characteristic of Rh–Rh bonds found in Rh carbonyl clusters.

From a comparison of the Rh–Rh distances in the tetrahedral $Rh_4(CO)_{12}$ and in the octahedral $Rh_6(CO)_{16}$ clusters (2.73 and 2.78 Å, respectively), it can be inferred that the latter is the best candidate. To support this tentative assignment, the experimental distribution (Fig. 1d) was compared with distributions calculated from the crystal data of rhodium carbonyl. Figures 4a and 4b give the distributions calculated for an isolated $Rh_6(CO)_{16}$ cluster and for "bulk" $Rh_6(CO)_{16}$, more precisely a 35 × 30 × 35-Å large fragment (12 unit cells). The latter exhibit peaks at $d > 6$ Å, which correspond to distances between pairs of $Rh_6(CO)_{16}$ entities. The experimental distribution (Fig. 1d) is intermediate between that of the isolated cluster (Fig. 4a) and that of "bulk" $Rh_6(CO)_{16}$ (Fig. 4b), since there are peaks near 8, 9, and 10 Å but they are much smaller than on distribution 4b. This means that a substantial fraction of $Rh_6(CO)_{16}$ clusters are associated and crystallize in aggregates. A rough estimate of the fraction can be obtained by comparing distributions calculated from different proportions of isolated and bulk rhodium carbonyl with the experimental distribution. Figure 5 gives the distribution calculated for a 70% fraction of isolated clusters. Comparison of this distribution (and of other distributions calculated for different fractions) with Fig. 1d allows us to conclude that more than two-thirds of the rhodium carbonyls are in the form of isolated species. Isolated clusters can be accommodated in the supercages. On the other hand clusters associated together can either occupy several adjacent supercages as observed previously (*24*) for Pd metal clusters, or agglomerate in dislocations of the zeolite lattice or at the bound-

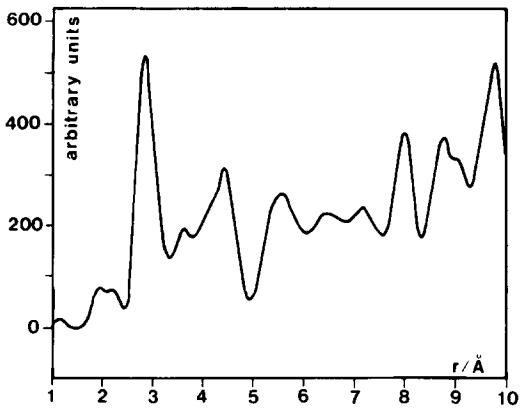

FIG. 5. Radial electron distribution calculated for a 70% fraction of isolated $Rh_6(CO)_{16}$ clusters and a 30% fraction of $Rh_6(CO)_{16}$ fragments (see Fig. 4).

ary between twinned zeolite crystals. A recent transmission electron microscopic study (*25*) of Rh and Ir zeolites provides clear evidence for metal aggregates filling inner voids present at lattice defects. These voids could also accommodate the associated carbonyl clusters.

The formation of these rhodium carbonyl clusters, either isolated or agglomerated, involves the transport of rhodium species, most probably the monomeric $Rh^I(CO)_2$, throughout the zeolite micropores. The continuous modifications of the X-ray pattern observed after $CO : H_2O$ additions (vide supra) is probably due to this migration which changes the distribution of the extra-framework scattering matter in the zeolite cages.

CONCLUSIONS

Two important results emerge from the present RED investigation.

(1) It is clearly demonstrated that Rh aggregates encaged in zeolites can be totally disintegrated upon CO adsorption at room temperature. This means that CO molecules extract and oxidize the Rh atoms from the aggregates and the $Rh^I(CO)_2$ monomeric species thus formed redisperse in neighboring cages. However, the process is not complete in the case of larger rhodium particles. Comparable oxidative disintegration, with a similar size dependence, occurs for the same metal on other supports. This is clear from the series of EXAFS studies on Rh/Al_2O_3 and Rh/TiO_2 (*9–12*). The fact that the process operates whatever the support seems to indicate that the dissociation of CO is involved as suggested previously (*11*). However, protons are available on alumina as well as on zeolite so that their role in the oxidation process cannot be discarded.

(2) It is also clearly demonstrated that the monomeric $Rh^I(CO)_2$ species coming from the oxidative disintegration of rhodium aggregates can condense into carbonyl clusters. From a comparison of experimental and calculated distributions it is concluded that $Rh_6(CO)_{16}$ clusters are synthesized both in an isolated form, which can be accommodated in the zeolite supercages, and in an agglomerated form which can be located in inner voids (fractures) of the zeolite lattice. The formation of $Rh_6(CO)_{16}$ in Y zeolites has also been observed by reacting $CO : H_2O$ mixtures on Rh^{III} cations (*18*). It proceeds *via* $Rh^I(CO)_2$ species which are therefore the necessary building blocks for the synthesis of rhodium carbonyl clusters. Similarly $Ir_6(CO)_{16}$ clusters have been synthesized by reaction of $CO : H_2O$ or $CO : H_2$ mixtures on Ir^{III} cations (*26*). In contrast with $Rh_6(CO)_{16}$, all the iridium clusters remain isolated.

For the first time the transformation of Rh metal aggregates into Rh carbonyl clusters is demonstrated. The different redox and transport processes operating under very mild conditions which are part of the driving force leading to a more stable configuration in the Rh–CO–zeolite system are under study.

ACKNOWLEDGMENTS

The computations of the experimental and model radial distributions were performed at Centre Inter Régional de Calcul Electronique (CIRCE, Orsay, France).

REFERENCES

1. Gallezot, P., Bienenstock, A., and Boudart, M., *Nouv. J. Chim.* **2,** 263 (1978).
2. Gallezot, P., and Bergeret, G., *J. Catal.* **72,** 294 (1981).
3. Gallezot, P., *J. Chim. Phys.* **78,** 881 (1981).
4. Gallezot, P., *Zeolites* **2,** 103 (1982).
5. Bergeret, G., and Gallezot, P., *J. Catal.* **87,** 86 (1984).
6. Che, M., Dutel, J. F., Gallezot, P., and Primet, M., *J. Phys. Chem.* **80,** 2371 (1976).
7. Kaufherr, N., Primet, M., Dufaux, M., and Naccache, C., *C.R. Acad. Sci. Paris Ser. C* **286,** 131 (1978).
8. Primet, M., *J. Chem. Soc. Faraday Trans. I* **74,** 2579 (1978).
9. van't Blik, H. F. J., van Zon, J. B. A. D., Huizinga, T., Vis, J. C., Koningsberger, D. C., and Prins, R., *J. Phys. Chem.* **87,** 2264 (1983).
10. van't Blik, H. F. J., van Zon, J. B. A. D., Koningsberger, D. C., and Prins, R., *J. Mol. Catal.* **25,** 379 (1984).
11. van't Blik, H. F. J., van Zon, J. B. A. D., Huizinga, T., Vis, J. C., Koningsberger, D. C., and Prins, R., *J. Amer. Chem. Soc.* **107,** 3139 (1985).
12. Koninsberger, D. C., van't Blik, H. F. J., van Zon, J. B. A. D., and Prins, R., *in* "Proceedings 8th International Congress on Catalysis, Berlin, 1984," Vol. 5, p. 123, Verlag Chemie, Weinheim, 1984.
13. Solymosi, F., and Pasztor, M., *J. Phys. Chem.* **89,** 4789 (1985).
14. Mantovani, F., Palladino, N., and Zanobi, A., *J. Mol. Catal.* **3,** 265 (1977–1978).
15. Smith, A. K., Hugues, F., Theolier, A., Basset, J. M., Ugo, R., Zanderighi, G. M., Bilhou-Bougnol, J. L., and Graydon, W. F., *Inorg. Chem.* **18,** 3105 (1979).
16. Gelin, P., Lefebvre, F., Elleuch, B., Naccache, C., and Ben Taarit, Y., *in* "Intrazeolite Chemistry" (G. D. Stucky and F. G. Dwyer, Eds.), *ACS Symposium Series* **218,** p. 455. Amer. Chem. Soc., Washington, DC, 1983.
17. Lefebvre, F., Gelin, P., Naccache, C., and Ben Taarit, Y., *in* "Proceedings 6th International Conference on Zeolites, Reno, 1983" (A. Bisio and D. H. Olson, Eds.), p. 435. Butterworth, Guildford, 1984.
18. Bergeret, G., Gallezot, P., Gelin, P., Ben Taarit, Y., Lefebvre, F., and Shannon, R. D., *Zeolites* **6,** 392 (1986).
19. Coey, J. M. D., *Acta Crystallogr. Ser. B* **26,** 1876 (1970).
20. Rogers, D. B., Shannon, R. D., Sleight, A. W., and Gillson, J. R., *Inorg. Chem.* **8,** 841 (1969).
21. Van Brabant, H., Schoonheydt, R. A., and Pelgrims, J., *in* "Metal Microstructures in Zeolites" (P. A. Jacobs, N. I. Jaeger, P. Jírů and G. Schulz-Ekloff, Eds.), Studies in Surface Science and Catalysis, Vol. 12, p. 61. Elsevier, Amsterdam, 1982.
22. Bergeret, G., and Gallezot, P., *in* "Proceedings 8th International Congress on Catalysis, Berlin, 1984," Vol. 5, p. 659. Verlag Chemie, Weinheim, 1984.
23. Gelin, P., Ben Taarit, Y., and Naccache, C., *in* "Proceedings 7th International Congress on Catalysis, Tokyo, 1980" (T. Seiyama and K. Tanabé, Eds.), p. 398. Kodansha/Elsevier, Tokyo/Amsterdam, 1981.
24. Bergeret, G., Gallezot, P., and Imelik, B., *J. Chem. Phys.* **85,** 411 (1981).
25. Gallezot, P., and Bergeret, G., *in* "Deactivation and Poisoning: Proceedings 3rd International Symposium on Catalysts, Berkeley, 1985" (E. E. Petersen and A. T. Bell, Eds.), p. 263. Dekker, New York, 1987.
26. Bergeret, G., Lefebvre, F., and Gallezot, P., *in* "New Developments in Zeolite Science Technology: Proceedings 7th International Zeolite Conference, Tokyo, 1986" (Y. Murakami, A. Iijima, and J. W. Ward, Eds.), p. 401. Kodansha, Tokyo, 1986.
27. D'Antonio, P., and Konnert, J. H., *J. Appl. Crystallogr.* **13,** 459 (1980).
28. Corey, E. C., Dahl, L. F., and Beck, W., *J. Amer. Chem. Soc.* **85,** 1202 (1963).